

Technical Notes

Attenuated Total Reflection Design for in Situ FT-IR Spectroelectrochemical Studies

Hendrik Visser,^{†,‡} Aimee E. Curtright,[‡] James K. McCusker,^{‡,§} and Kenneth Sauer^{*,†,‡}

Melvin Calvin Laboratory, Physical Biosciences Division, Lawrence Berkeley National Laboratory, Berkeley, California 94720-5230, and Department of Chemistry, University of California, Berkeley, California 94720-5230

A versatile spectroelectrochemical apparatus is introduced to study the changes in IR spectra of organic and inorganic compounds upon oxidation or reduction. The design is based on an attenuated total reflection device, which permits the study of a wide spectral range of 16 700 (600 nm)–250 cm^{−1}, with a small opaque region of 2250–1900 cm^{−1}. In addition, an IR data collection protocol is introduced to deal with electrochemically nonreversible background signals. This method is tested with ferrocene in acetonitrile; concentrations as low as 1 mM produce results that agree with those in the literature.

In situ FT-IR spectroelectrochemistry has proven useful for elucidating the structure of chemical intermediates and studying the redox chemistry of a wide range of molecules. In the past, many in situ infrared spectroelectrochemistry designs have been proposed and developed.^{1–4} These designs range from transmission electrochemical cells to designs utilizing reflectance methods. Transmission electrochemical cells, using minigrid electrodes, measure the IR features of the electrochemical species in bulk solution.^{5–10} In contrast, most reflectance methods measure the IR features of the electrochemical species near or on the electrode surface, with either totally reflective^{11–13} or transparent^{14–17} electrodes. Each of these approaches has addressed the problem

of absorption of IR radiation by the solvent, but most designs do have other problems associated with them. For example, minigrid electrodes have scatter problems, and thin-cell transmittance designs in general are sensitive to leakage and difficult to purge of oxygen. Because reflectance methods have measured the electrochemical species near and on the electrodes, their spectra can differ from the species in the bulk solution.^{18–20} In addition, transparent electrodes, which are used in attenuated total reflection (ATR) devices, generally have specific IR features, which can block important spectral regions.^{13–17,21,22}

A versatile in situ infrared spectroelectrochemistry design is presented with a wide spectral range: 16 700–2250 and 1900–250 cm^{−1}. It requires a small total sample volume (0.7 mL) which can be purged easily. The design is resistant to a variety of solvents, and different types of electrodes can be utilized. Good signal-to-noise ratios are obtained for concentrations of ferrocene as low as 1 mM. The design is based on an ATR device that was developed for following chemical reactions in situ using FT-IR spectroscopy.^{23,24} This device is modified to perform preparative electrochemistry, permitting measurement of the IR spectrum of the bulk solution near an ATR window. In contrast to previous spectroelectrochemical ATR devices,^{14–16,21,22} the working elec-

* To whom correspondence should be addressed. Tel: (510) 486-4334. Fax: (510) 486-6059. e-mail: KHSauer@LBL.GOV.

† Lawrence Berkeley National Laboratory.

‡ University of California, Berkeley.

§ Present address: Department of Chemistry, Michigan State University, East Lansing, MI 48824.

- (1) Heineman, W. R. *J. Chem. Educ.* **1983**, *60*, 305–308.
- (2) Ashley, K. *Talanta* **1991**, *38*, 1209–1218.
- (3) Foley, J. K.; Pons, S. *Anal. Chem.* **1985**, *57*, 945A–956A.
- (4) Korzeniewski, C. *Crit. Rev. Anal. Chem.* **1997**, *27*, 81–102.
- (5) Hartl, F.; Luyten, H.; Nieuwenhuis, H. A.; Schoemaker, G. C. *Appl. Spectrosc.* **1994**, *48*, 1522–1528.
- (6) Krejcik, M.; Danek, M.; Hartl, F. *J. Electroanal. Chem.* **1991**, *317*, 179–187.
- (7) Flowers, P. A.; Mamantov, G. *Anal. Chem.* **1989**, *61*, 190–192.
- (8) Yao, C.-L.; Capdevielle, F. J.; Kadish, K. M.; Bear, J. L. *Anal. Chem.* **1989**, *61*, 2805–2809.
- (9) Nevin, W. A.; Lever, A. B. P. *Anal. Chem.* **1988**, *60*, 727–730.
- (10) Bullock, J. P.; Boyd, D. C.; Mann, K. R. *Inorg. Chem.* **1987**, *26*, 3084–3086.
- (11) Rosa-Montañez, M. E.; De Jesús-Cardona, H.; Cabrera-Martínez, C. R. *Anal. Chem.* **1998**, *70*, 1007–1011.

- (12) Klíma, J.; Kratochvílová, K.; Ludvík, J. *J. Electroanal. Chem.* **1997**, *427*, 57–61.
- (13) Best, S. P.; Clark, R. J. H.; McQueen, R. C. S.; Cooney, R. P. *Rev. Sci. Instrum.* **1987**, *58*, 2071–2074.
- (14) Kulesza, P. J.; Malik, M. A.; Denca, A.; Strojek, J. *Anal. Chem.* **1996**, *68*, 2442–2446.
- (15) Ping, Z.; Neugebauer, H.; Neckel, A. *Electrochim. Acta* **1996**, *41*, 767–772.
- (16) Bae, I. T.; Sandifer, M.; Lee, Y. W.; Tryk, D. A.; Sukenik, C. N.; Scherson, D. A. *Anal. Chem.* **1995**, *67*, 4508–4513.
- (17) Neugebauer, H.; Nauer, G.; Brinda-Konopik, N.; Gidaly, G. *J. Electroanal. Chem.* **1981**, *122*, 381–385.
- (18) Huang, J.; Barham, M. D.; Korzeniewski, C. *Microchem J.* **1999**, *62*, 114–120.
- (19) Korzeniewski, C.; Shirts, R. B.; Pons, S. *J. Phys. Chem.* **1985**, *89*, 2297–2298.
- (20) Schmidt, P. P.; Seversen, M.; Korzeniewski, C.; Pons, S. *J. Electroanal. Chem.* **1987**, *225*, 267–272.
- (21) Hansen, W. N.; Kuwana, T.; Osteryoung, R. A. *Anal. Chem.* **1966**, *38*, 1810–1821.
- (22) Hansen, W. N.; Osteryoung, R. A.; Kuwana, T. *J. Am. Chem. Soc.* **1966**, *88*, 1062–1063.
- (23) Sheridan, R. E.; Rein, A. J. *R&D* **1991**, *33*, 100–102.
- (24) Milosevic, M.; Sting, D.; Rein, A. *Spectroscopy* **1995**, *10*, 44–49.

trode is separate from the sensing window. Therefore, this design measures the IR features of the electrochemical species in bulk solution.²⁵ The system is tested with ferrocene, and the resulting IR spectra are compared to spectra previously published using transmission electrochemical cells.^{6,10} The system has been successfully applied to analysis of nanosecond IR spectra of a series of substituted $[\text{Ru}(\text{bpy})_3]^{2+}$ complexes. Transient MLCT excited-state IR features were identified by comparison with oxidized and reduced species.²⁶ In addition, this method has been used to study changes in the vibrational features of $[\text{Mn}_4\text{O}_6(\text{bpea})_4]^{4+}$ on reduction, at concentrations of $\sim 2 \text{ mM}$.²⁷

METHODS

Spectroelectrochemical Apparatus. The spectroelectrochemical apparatus consists of a home-built electrochemical cell designed to interface with an ASI DuraSamplIR ATR accessory (Applied Systems Inc., Annapolis, MD). The IR beam passes through a KRS-5 support element and a 3-mm diamond sensing window of the ATR device, providing a wide spectral range of $16\,700\text{--}250\text{ cm}^{-1}$, with a small opaque region of $2250\text{--}1900\text{ cm}^{-1}$. Figure 1A shows the electrochemical cell, including the clamp that attaches the cell to the stainless steel interface plate of the ATR device. The electrochemical cell, constructed from a Teflon disk, is bolted to the clamp. A slot is excavated from this disk to make space for the reference and auxiliary electrodes, and a small circular cavity inside this groove provides contact between bulk solution and diamond sensing window. Figure 1B gives a side view of the cell along the long axis of the slot in the disk, which requires a sample volume of $\sim 0.7 \text{ mL}$. A seal between the Teflon disk and interface plate of the ATR device is provided by a butyl O-ring (resistant to acetonitrile).

Electrochemistry. The working electrode consists of a Pt wire lead (0.5-mm diameter) connected to a 6-mm-diameter disk of Pt gauze (52 mesh woven of 0.1-mm-diameter wire). The auxiliary electrode is similarly constructed with Pt gauze and is placed inside a glass tube with a fritted glass disk at the end to allow electrochemical contact while minimizing diffusion of electrochemical products. A nonaqueous (CH_3CN , 0.1 M $\text{TBA}(\text{PF}_6)$) Ag/AgClO_4 reference electrode is used ($+270 \text{ mV}$ more positive than SCE). This electrode is isolated from the bulk solution by an additional electrolyte bridge (a glass tube with a Vycor tip), which is changed between samples to avoid contamination (Figure 1B). The interface plate of the ATR accessory is grounded by connection to the ground of the voltammeter.

The electrolyte solution (0.1 M $\text{TBA}(\text{PF}_6)$ in acetonitrile) is dried over Al_2O_3 , bubbled with Ar and kept under a constant flow of Ar throughout the experiment. To minimize evaporation and the resultant change in electrolyte and ferrocene concentration, the Ar is bubbled through dry CH_3CN (Al_2O_3). Ferrocene is obtained from Aldrich. The electrochemistry is conducted using a BAS CV-27 voltammetry controller. Oxidation of the ferrocene is performed at $+0.33 \text{ V}$ and reduction at -0.67 V vs SCE ($E_{1/2}[\text{ferrocene}] = -0.17 \text{ V}$ vs SCE).

FT-IR Spectroscopy. The FT-IR spectra are collected using a Bruker IFS88 FT-IR spectrometer, with a broad-band MCT

(25) Horton, J. A.; Hansen, W. N. *Anal. Chem.* **1967**, *39*, 1097–1100.

(26) Curtright, A. E.; McCusker, J. K. *J. Phys. Chem. A* **1999**, *103*, 7032–7041.

(27) Visser, H.; Dubé, C. E.; Armstrong, W. H.; Sauer, K.; Yachandra, V. K. Manuscript in preparation.

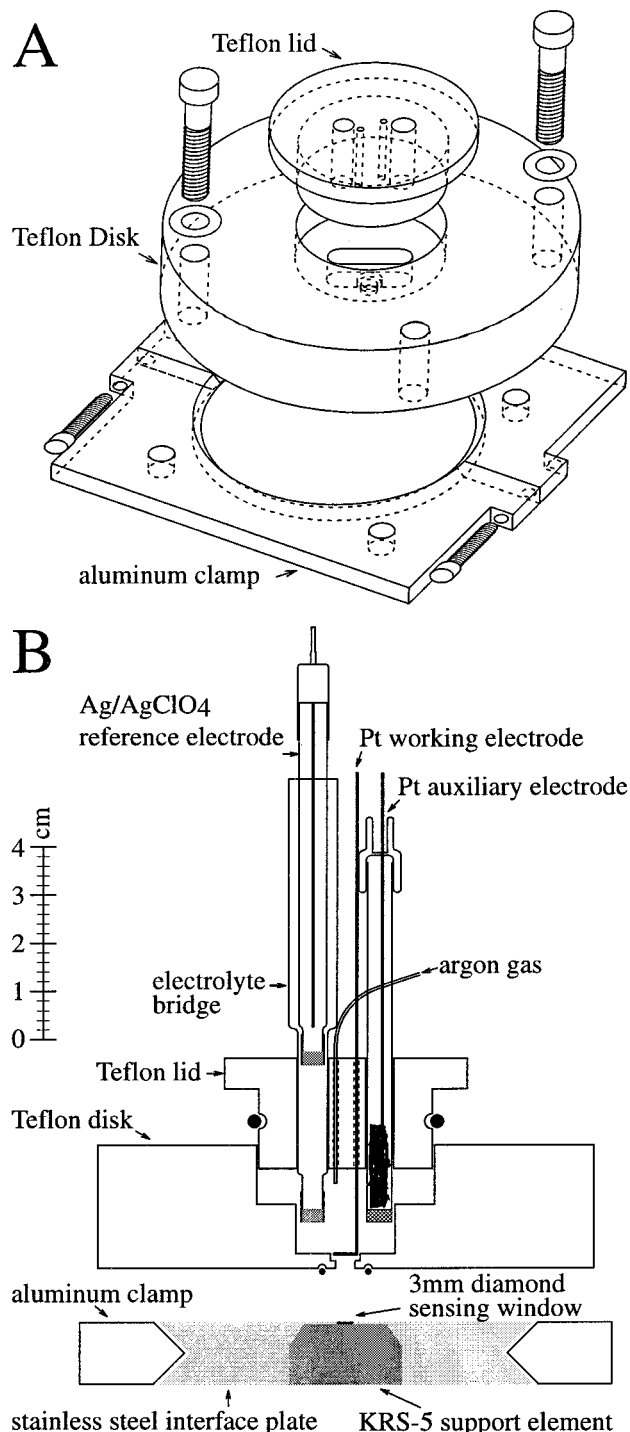


Figure 1. (A) Electrochemical cell designed to fit onto the ASI DuraSamplIR ATR accessory, consisting of an aluminum base clamp, a Teflon disk from which the cell compartment is excavated and a Teflon, airtight lid. (B) Cross section of the cell along the long axis of the excavated slot. The total sample volume required is $\sim 0.7 \text{ mL}$.

detector (lower cutoff 400 cm^{-1}). Before each experiment, the absorption spectrum is checked at the 1375 and 1038-cm^{-1} acetonitrile peaks; if the values are not ~ 0.13 and ~ 0.09 , respectively, the working electrode is adjusted to remove air bubbles that are trapped on the diamond window below the working electrode. All spectra are taken at a resolution of 4 cm^{-1} , and absorption spectra consist of 100 averaged scans. Spectra taken during electrochemistry are recorded in rapid-scan mode

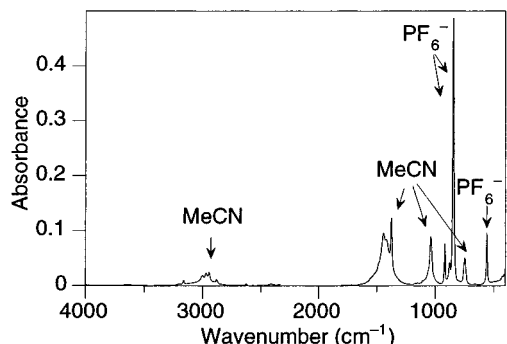


Figure 2. FT-IR absorption spectrum of 5 mM ferrocene, 0.1 M TBA(PF₆) in acetonitrile solution before electrochemistry (average of 100 scans at 4-cm⁻¹ resolution).

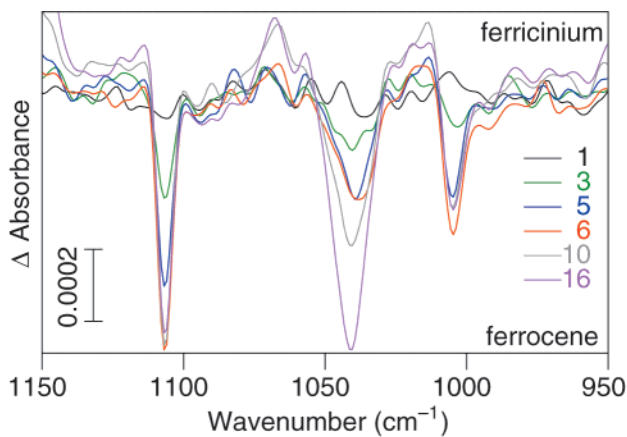


Figure 3. FT-IR difference spectra at different times during the oxidation of a 5 mM ferrocene, 0.1 M TBA(PF₆) in acetonitrile solution. The numbers refer to the scan group taken after starting the electrochemistry (each scan group is 1.28 s), which are subtracted against one scan group taken before electrochemistry at a 4-cm⁻¹ resolution. For both the oxidation and reduction difference spectra, negative features are due to disappearance (oxidation) or appearing (reduction) of ferrocene and the positive features are due to appearing (oxidation) or disappearing (reduction) of ferricinium.

(128 ms/scan) and 100 scans are averaged into a scan group (12.8 s).

RESULTS AND DISCUSSION

Figure 2 shows the FT-IR absorption spectrum of a 5 mM ferrocene electrolyte solution in the spectroelectrochemical cell, which is dominated by the bulk solvent and electrolyte. Characteristic peaks of ferrocene, such as those at 1107 and 1005 cm⁻¹, are too small to be observed. Therefore, it is necessary to obtain difference spectra of the solution before and after electrochemistry.

Figure 3 shows the FT-IR absorption difference spectra during the oxidation (Fe^{II} to Fe^{III}) of a 5 mM ferrocene solution, 0.1 M TBA(PF₆) in acetonitrile. A decrease of the ferrocene peaks at 1107 and 1005 cm⁻¹ can be observed as a function of time (corresponding to scan-group number in Figure 3) after starting the oxidation. The signals associated with the oxidation of ferrocene attain their maximum after roughly six scan groups (600 scans or ~80 s). When electrochemistry is performed on low concentrations of electrochemical species, certain background signals occur, such as at 1040 cm⁻¹. These bands can be

distinguished here due to their different dynamic behavior relative to those associated with ferrocene. In addition, these background signals also are electrochemically nonreversible.

Based on these differences of the signals, an experimental procedure is performed where IR spectra are taken while alternating between oxidation and reduction periods. This enables us to make a distinction between reversible signals, which oscillate with the oxidation and reduction periods, and nonreversible signals which do not oscillate. In this case, reversible signals are expected from the electrochemically active ferrocene/ferricinium couple and the nonelectrochemically active counterion, PF₆⁻. The reversible IR signal of the counterion, PF₆⁻, is due to the fact that the solution needs to stay charge neutral. Consequently, when ferrocene is oxidized into ferricinium, the local concentration of PF₆⁻ increases. These counterions come from the counter electrode, where the opposite reaction occurs, and the PF₆⁻ concentration decreases. Nonreversible signals are due to reactions of the solvent or electrolyte at the working electrode or decomposition products of ferrocene/ferricinium.

The electrochemical periods, consisting of 16 scan groups (~205 s), are chosen to minimize the rise of the solvent signals, while maximizing the ferrocene/ferricinium signal. To obtain the oxidation difference spectra, the last 12 scan groups before oxidation of ferrocene are averaged and subtracted from the average of scan groups 5–16 after oxidation ([av scan groups 5–16]_{before ox} – [av scan group 5–16]_{after ox} = oxidation spectrum). The reduction spectra are obtained by subtracting the average of scan groups 5–16 after reduction of ferricinium from the last 12 scan groups just before the reduction starts ([av scan groups 5–16]_{after red} – [av scan group 5–16]_{before red} = reduction spectrum). For both the oxidation and reduction difference spectra, negative features are due to disappearance (oxidation) or appearance (reduction) of ferrocene, and the positive features are due to appearance (oxidation) or disappearance (reduction) of ferricinium. The first four scan groups of each redox period are not used because of their small ferrocene/ferricinium signal contribution. In Figure 4, each panel shows the difference spectra obtained for the first oxidation (purple) and reduction (blue). Reversible features have the same sign in both the oxidation and reduction spectra, and nonreversible features have the opposite sign. Reversible features are indicated with arrows. Two types of nonreversible features occur in Figure 4, which can be distinguished by their different dynamic behavior. The features at 840 and 550 cm⁻¹ are due to the counterion PF₆⁻ (see also Figure 2). These are the only two features that occur when no potential is applied to an electrolyte solution, i.e., without ferrocene present. As mentioned above, these signals are expected to be reversible, because PF₆⁻ is the counterion to the ferrocene/ferricinium couple. Even though great care is taken to prevent evaporation of acetonitrile, a constant increase in concentration is observed, which overwhelms the reversible behavior of the counterion features. (Reversibility of the PF₆⁻ IR signal has been observed in other experiments.) However, when a potential is applied to the electrolyte solution, the nonreversible signals at 2900, 1478, 1040, and 740 cm⁻¹ occur, indicating that these nonreversible features are due to decomposition of the electrolyte solution. Similar IR features have been observed for acetonitrile solutions, with TBA(BF₄) and TPA(BF₄) as the electrolyte, at higher and

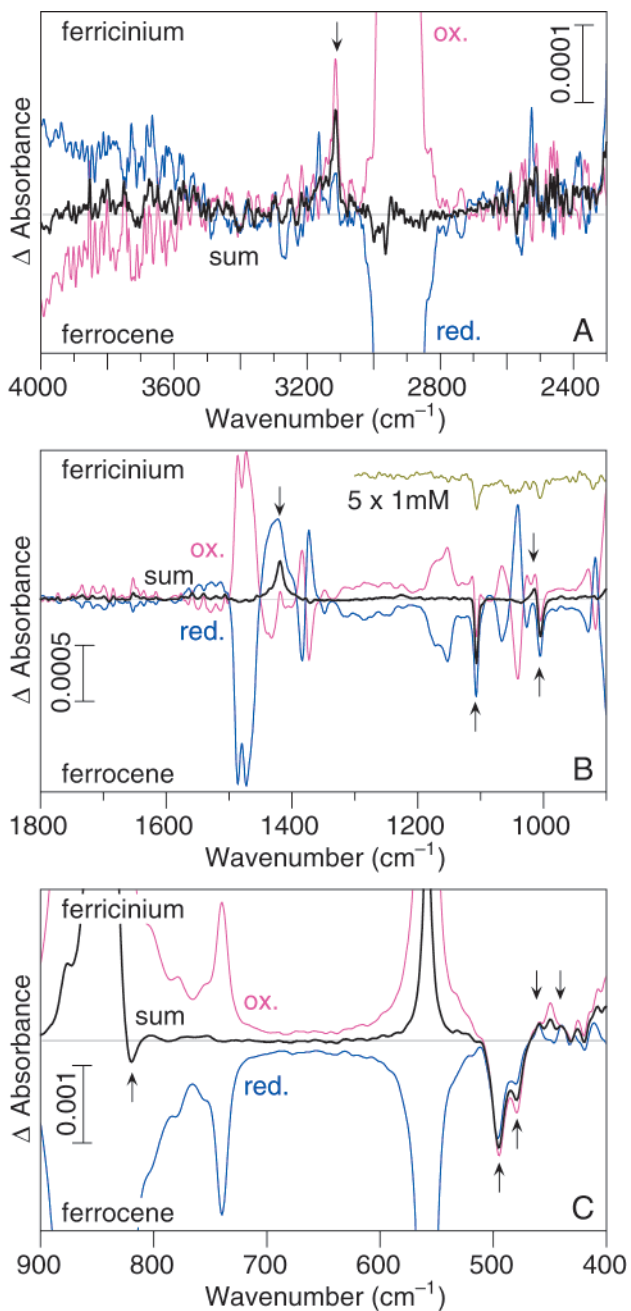


Figure 4. FT-IR difference spectra of ferricinium/ferrocene, of a 5 mM ferrocene, 0.1 M TBA(PF_6^-) acetonitrile solution for three spectral regions. Each graph shows difference spectra of the first oxidation (purple) step, first reduction (blue) step, and the averaged sum of two oxidations and two reduction steps (black). Arrows indicate reversible absorption peaks that can be ascribed to either ferrocene or ferricinium. Spectra are taken at 4- cm^{-1} resolution. For both the oxidation and reduction difference spectra, negative features are due to disappearing (oxidation) or appearing (reduction) of ferrocene, and the positive features are due to appearing (oxidation) or disappearing (reduction) of ferricinium.

lower redox potentials.^{28–30} Additionally, all these features are underneath electrolyte absorption peaks (see also Figure 3).

(28) Foley, J. K.; Korzeniewski, C.; Pons, S. *Can. J. Chem.-Rev. Can. Chim.* **1988**, *66*, 201–206.
 (29) Pons, S.; Khoo, S. B. *Electrochim. Acta* **1982**, *27*, 1161–1169.
 (30) Portis, L. C.; Roberson, J. C.; Mann, C. K. *Anal. Chem.* **1972**, *44*, 294–297.

Therefore, these nonreversible features are most likely due to changes of the electrolyte solution.

Each oxidation and reduction is performed twice, and the oxidation and reduction spectra are averaged. The sum spectrum (black) is obtained by subtracting a fraction (F) of the averaged reduction spectrum from the oxidation spectrum (av ox spectrum – $F \times$ av red spectrum = sum spectrum). F is chosen so that all nonreversible features due to the acetonitrile are minimized over the whole spectral range. For the sum spectrum in Figure 4, F is 0.82. The sum spectrum shows several signals due to the ferrocene/ferricinium species. Upon oxidation of ferrocene, new vibrational features appear at 3114, 1419, 1014, 458, and 440 cm^{-1} . Vibrational features at 1107, 1005, 819, 494, and 479 cm^{-1} disappear due to the formation of ferricinium. The difference features at 1107, 1014, and 1005 cm^{-1} agree with previously published data,^{6,10,11} indicating that this spectroelectrochemical design and method of data acquisition is capable of measuring low concentrations of electrochemical species. To the knowledge of the authors, this is the first time that the IR difference features at 3114, 1419, 819, 494, 479, 458, and 440 cm^{-1} have been observed and assigned to vibrational changes of ferrocene when oxidized into ferricinium. The inset of Figure 4B shows the sum difference spectrum for a 1 mM ferrocene solution. Even though the spectrum is noisy, the two features at 1107 and 1005 cm^{-1} can be observed. With more signal-to-noise averaging, i.e., averaging more oxidation and reduction periods, one could presumably go to even lower concentrations.

CONCLUSIONS

Figure 4 shows that FT-IR difference spectra of the ferrocene/ferricinium couple, with concentrations as low as 1 mM, can be obtained using the spectroelectrochemical design. It is expected that with more data averaging one could go to even lower concentrations. The sensitivity of the method is enhanced by applying the experimental protocol of alternation between oxidation and reduction periods, which enables us to deal with electrochemically nonreversible background signals. Consequently, this spectroelectrochemical cell and data collection protocol could be useful for studying the electrochemical species of compounds with a low solubility.

Recently, this spectroelectrochemical design has been used in the analysis of a variety of inorganic complexes. It has been successfully applied to identify features in IR spectra of asymmetrically substituted $[\text{Ru}^{\text{II}}(\text{bpy})_3]^{2+}$ -type complexes at concentrations of 5–10 mM.²⁶ IR features that correspond to $(\text{Ru}^{\text{III}}(\text{bpy}))$ and reduced ligand ($\text{bpy}^{\text{-}}$) were identified by comparison of the spectra from the nanosecond transient MCLT excited-state IR with that of the electrochemically prepared species. In addition, this method has been used to study the vibrational features of $[\text{Mn}_4\text{O}_6(\text{bpea})_4]^{4+}$ and the reduced species, at concentrations of \sim 2 mM.²⁷

A drawback of this design is that the response time of the compound signal is dependent on the rate of diffusion. Therefore, the dynamic behavior during electrochemistry is dependent on the size of the studied compound and the distance between working electrode and sensing window. Due to the diffusion limitations, it is likely that not all the ferrocene/ferricinium in solution is oxidized or reduced within the redox periods. Consequently, the IR features of the ferrocene/ferricinium couple do not attain the maximal intensities possible. To eliminate the

diffusion dependence, the bulk solution needs to be stirred. When the solution is stirred, it is expected that the overall electrochemistry will be accelerated and be more complete; as a result the signal-to-noise ratio improves. Stirring of the solution will also help reduce the background signal problems, because the redox periods can be shortened. To facilitate this enhancement, a stir rod could be added through the Teflon lid and a basket-shaped working electrode could be used instead of a disk-shaped one. Several other permutations of the cell can be envisioned. For example, the total volume could be reduced using reference and auxiliary microelectrodes. The Pt working electrode could be of another electrode material, for example, reticulated vitreous carbon. If experiments at a lower temperature are required, a cooling jacket could be added in the Teflon disk around the cell groove (the ASI DuraSamplIR ATR accessory is stated to give reproducible results down to ~ 230 K). The flexibility of our design allows for these and other modifications.

Abbreviations: ATR, attenuated total reflection; IR, infrared; FT-IR, Fourier transform infrared; MCT, mercury–cadmium–

telluride; ox, oxidation; red, reduction; bipy, 2,2'-bipyridine; bpea, *N,N*-bis(2-pyridylmethyl)ethylamine; TBA, *tert*-butylammonium; TPA, *tert*-*n*-propylammonium; MeCN, acetonitrile; MLCT, metal-to-ligand charge transfer.

ACKNOWLEDGMENT

The authors thank Dr. Heinz Frei for the use of Bruker IFS88 FT-IR spectrometer and Dr. Elodie Anxolabéhère-Mallart for helpful discussions. This research was supported by the U.S. Department of Energy, Office of Basic Energy Sciences, Division of Chemical Sciences (Grant DE-FG03-96ER14665) and Division of Energy Biosciences (Grant DE-AC03-76SF00098), National Institutes of Health (Grant GM 55302), American Chemical Society Petroleum Research Fund (Grant 31016-G6), and the Alfred P. Sloan Foundation.

Received for review February 7, 2001. Accepted June 27, 2001.

AC010167Q